Materials Science and Engineering A 526 (2009) 113–117

Contents lists available at ScienceDirect

Materials Science and Engineering A

journal homepage: www.elsevier.com/locate/msea

Friction stir welding of titanium alloy TiAl6V4 to aluminium alloy AA2024-T3

Ulrike Dressler*, Gerhard Biallas[1], Ulises Alfaro Mercado

German Aerospace Center, Institute of Materials Research, Linder Höhe, 51147 Köln, Germany

ARTICLE INFO

Article history:
Received 5 March 2009
Received in revised form 1 July 2009
Accepted 2 July 2009

Keywords:
Friction stir welding
Titanium
Aluminium

ABSTRACT

Titanium alloy TiAl6V4 and aluminium alloy 2024-T3 were successfully joined by friction stir welding. Microstructure, hardness and tensile strength of the butt joint were investigated. The weld nugget exhibits a mixture of fine recrystallized grains of aluminium alloy and titanium particles. Hardness profile reveals a sharp decrease at titanium/aluminium interface and evidence of microstructural changes due to welding on the aluminium side. The ultimate tensile strength of the joint reached 73% of AA2024-T3 base material strength.

1. Introduction

Highest performance and concurrent weight and cost reduction become more and more important in aviation industry. There are different approaches to meet these demands. It is well known, for example, that welding of skin-stringer joints is progressively replacing riveted fuselage structures [1]. Another very effective possibility is the implementation of hybrid structures; components made of different materials can be tailored to the local needs. As an implication there is need for a welding method allowing for joining dissimilar materials, such as titanium (corrosive properties, strength) and aluminium (low weight, low cost).

Several approaches to weld titanium to aluminium have been made in the past. Wilden and Bergmann [2] reported on diffusion welding between titanium alloys and aluminium alloys. They achieved sound joints applying temperatures of at least 480 °C over 45 min in a vacuum chamber. Electron beam welding was used to produce lap joints [3]; Osokin showed that fusion welding could join dissimilar materials if two separate weld pools were formed. Aluminium–titanium-tailored blanks were produced by laser processing [4]. The focused laser beam was shifted from the abutting edges of both sheets towards the titanium sheet. Both electron beam welding and laser processing need shielding gas to minimize oxidation. Friction welding might be a possibility to avoid the need for shielding gas. Fuji [5] joined dissimilar rods of 30 mm diameter and examined the growth of the intermediate layer.

All these representative examples revealed several problems like the necessity for shielding gas, sophisticated equipment and geometrical limitations of the joining pieces. Friction stir welding (FSW) patented by TWI [6] can solve these problems since it is a solid state joining process. This welding process is based on a quite simple concept: A non-consumable rotating welding tool is plunged into adjoining parent materials. Frictional heat generated by the tool shoulder during this process causes the materials to soften and local plastic deformation to occur. The softened material is stirred together by the rotating tool pin resulting in a solid state bond. Chen and Nakata [7] reported on friction stir lap welding between aluminium alloy and pure titanium, reaching a maximum failure load of 62% of the aluminium base material strength. The objective of this work is to demonstrate the feasibility to produce dissimilar butt joints of TiAl6V4 and AA2024-T3 by FSW and their characterization in terms of mechanical properties and microstructure.

2. Experimental details

Two millimetres thick sheets of titanium alloy TiAl6V4 and aluminium alloy 2024-T3 were successfully friction stir welded on the basis of the TWI patent [6] using an FSW adapted milling machine at German Aerospace Center. The nominal chemical composition of the materials is given in Table 1. The butt joints were welded using a FSW tool consisting of a threaded and tapered pin of 6 mm diameter and a concave shoulder of 18 mm diameter. The tool was made of standard tool steel and both the shoulder and the pin were coated to avoid excessive wear. Based on the standard parameters of similar AA2024 joints (850 rpm, 300 mm/min), the optimum parameters were found to be 800 rpm for tool rotation speed and 80 mm/min for

* Corresponding author. Tel.: +49 2203 601 2554; fax: +49 2203 696480.
E-mail addresses: ulrike.dressler@dlr.de (U. Dressler), gerhard.biallas@haw-hamburg.de (G. Biallas), ulises.alfaro@dlr.de (U. Alfaro Mercado).
[1] Present address: HAW Hamburg, Institut für Werkstoffkunde und Schweißtechnik, Berliner Tor 5, 20099 Hamburg, Germany.

0921-5093/$ – see front matter © 2009 Elsevier B.V. All rights reserved.
doi:10.1016/j.msea.2009.07.006

Table 1
Chemical composition limits.

	Si	Fe	Cu	Mn	Mg	Cr	Zn	Ti	V	Al
TiAl6V4	–	Max. 0.25	–	–	–	–	–	Bal.	3.5–4.5	5.5–6.75
AA 2024	Max. 0.50	Max. 0.50	3.8–4.9	0.30–0.9	1.2–1.8	Max. 0.10	Max. 0.25	Max. 0.15	–	Bal.

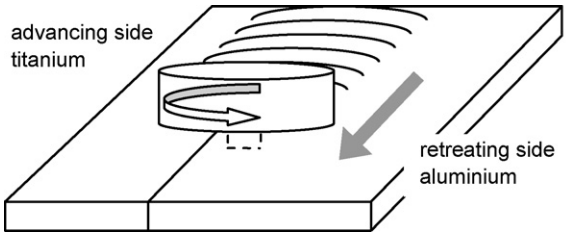

Fig. 1. Schematic illustrating friction stir welding of titanium–aluminium joints.

travel speed. Fig. 1 shows a schematic illustrating friction stir butt welding of dissimilar materials. Contrary to conventional friction stir butt welding, the tool pin centre was nearly shifted by the pin radius towards the aluminium plate, which was fixed on the retreating side. Therefore, except a few tenth of a millimetre, the stirring action of the pin happened in the aluminium part of the joint. This was done to prevent pin erosion and over-heating of the aluminium alloy. The process was similar to the FSW of steel–aluminium joints presented in [8–10].

The as-welded microstructure of the weld seam was inspected by optical microscopy; sections taken perpendicular to the welding direction were polished and etched using conventional methods. Hardness tests were done every 300 μm using a Vickers indenter and a load of 0.3 kg. Six specimens taken from two different sheets were tensile tested using an INSTRON 4505 screw driven test machine. At four specimens, the strain was measured by a FIEDLER laser extensometer, which allows to reveal local deformation in the different weld zones [11]; 0.2 mm were removed by milling from the lower surface of the tensile test specimens to eliminate the root flaw possibly occurring, so that the behaviour of titanium–aluminium joints without defects could be investigated. Furthermore, both polished metallographic cross-sections and fracture surfaces were examined by a scanning electron microscope (SEM) equipped with an energy-dispersive X-ray spectroscopy analysis system (EDX).

3. Results and discussions

Fig. 2 shows a macroscopic overview of the as-welded cross-section of the dissimilar friction stir welded joints of TiAl6V4 and AA2024-T3. Because the welding tool was shifted towards the Al alloy, the stirred zone (SZ) occurs mainly on the Al side of the joint. The SZ reveals a mixture of fine recrystallized grains of Al alloy and titanium particles pushed away from the titanium surface by the stirring action of the tool pin. Therefore the SZ has a composite structure of Al alloy reinforced by titanium particles. On the retreating side the SZ is followed by the thermo-mechanically affected zone (TMAZ) and the heat affected zone (HAZ) just like in conventional FSW-joints [12–14]. On the advancing titanium side of the joint, these zones do not occur. Nevertheless, next to the titanium–aluminium interface, a narrow band is observed, where the equiaxed primary α and transformed β grains have been elongated and rotated up to 90°, and grain size has been reduced remarkably. The width of this band varies between ca. 3–4 μm (Fig. 3) in the lower part of the welding and ca. 10 μm (Fig. 4) in the upper part. Combined influence of temperature and plastic deformation induced by the stirring action suggests a recrystallized structure (Fig. 5). Recrystallization in the small affected band is corroborated by the disappearance of remaining lamellar structures that have been found in the parent titanium alloy [15]. Aside from the small deformed band the titanium structure seems to be unaffected, because no further difference to titanium base material in microstructure or hardness can be observed. The interface between titanium and aluminium is properly bonded, apart from a small root flaw of circa 40 μm, maximum 70–80 μm height.

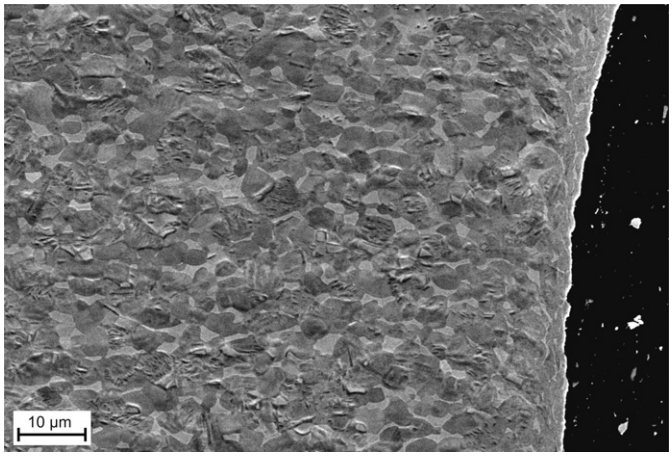

Fig. 3. Microstructure of titanium next to the aluminium–titanium interface, lower part (SEM-picture).

The hardness level (Fig. 6) continuously amounts to circa 330 HV0.3 on the titanium side. A sharp decrease to approximately

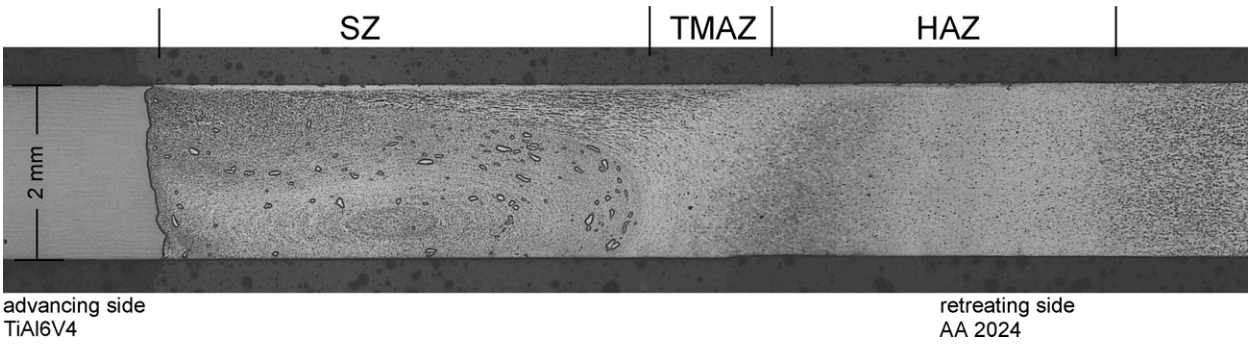

Fig. 2. Macrograph of FSW titanium–aluminium joint taken perpendicular to welding direction.

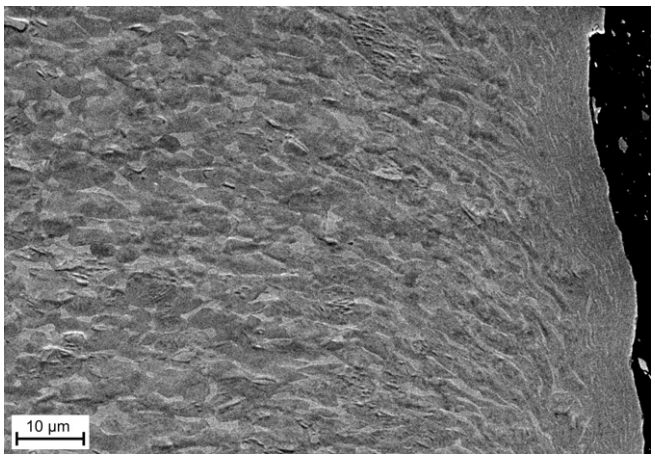

Fig. 4. Microstructure of titanium next to the aluminium–titanium interface, upper part (SEM-picture).

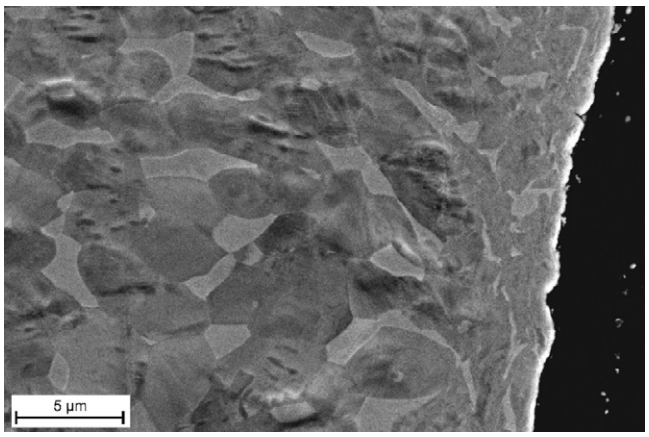

Fig. 5. Microstructure of titanium next to the aluminium–titanium interface.

140 HV0.3 occurs at the titanium/aluminium transition. On that level the hardness profile is proceeding on the retreating side (aluminium side) in principle like in conventional FSW-joints [16], except individual higher hardness values in the SZ, which occurred when the indenter hit a titanium particle (see inset picture in Fig. 6). The loss in hardness to a minimum of 117 HV0.3 (point A in Fig. 6) is caused by the relatively high heat input, which leads to an overaging effect. In spite of the high FSW process temperature, hardness values in the SZ reach 135–140 HV0.3. Probably, this is a result of grain boundary hardening (Hall-Petch effect) [17–19]. In areas of sufficient distance to the SZ, i.e. with minor effect of temperature, base material hardness values are observed. Compared to the present hardness profile, there are higher hardness values in both the SZ and the HAZ in optimized similar FSW-joints made from AA2024-T3 [11,12,18,20,21]. This can be rationalized by the excessive heat input that was generated on the aluminium side of the joint when adapting the process parameters to the conditions needed for welding aluminium to titanium.

The ultimate tensile strength of the friction stir welded titanium–aluminium joints reached 348 MPa (standard deviation = 7.67 MPa) representing 73% of the ultimate tensile strength of Al 2024-T3 base material (Fig. 7). Irrespective of the different strain to fracture ε_f, the stress–strain curves of the present dissimilar joint and AA2024-T3 base material shown in Fig. 7 are very similar. Thus, plastic elongation only took place on the aluminium side of the joint. Development of local strain obtained by laser extensometry [11] reveals a narrow deformation peak in the TMAZ/HAZ transi-

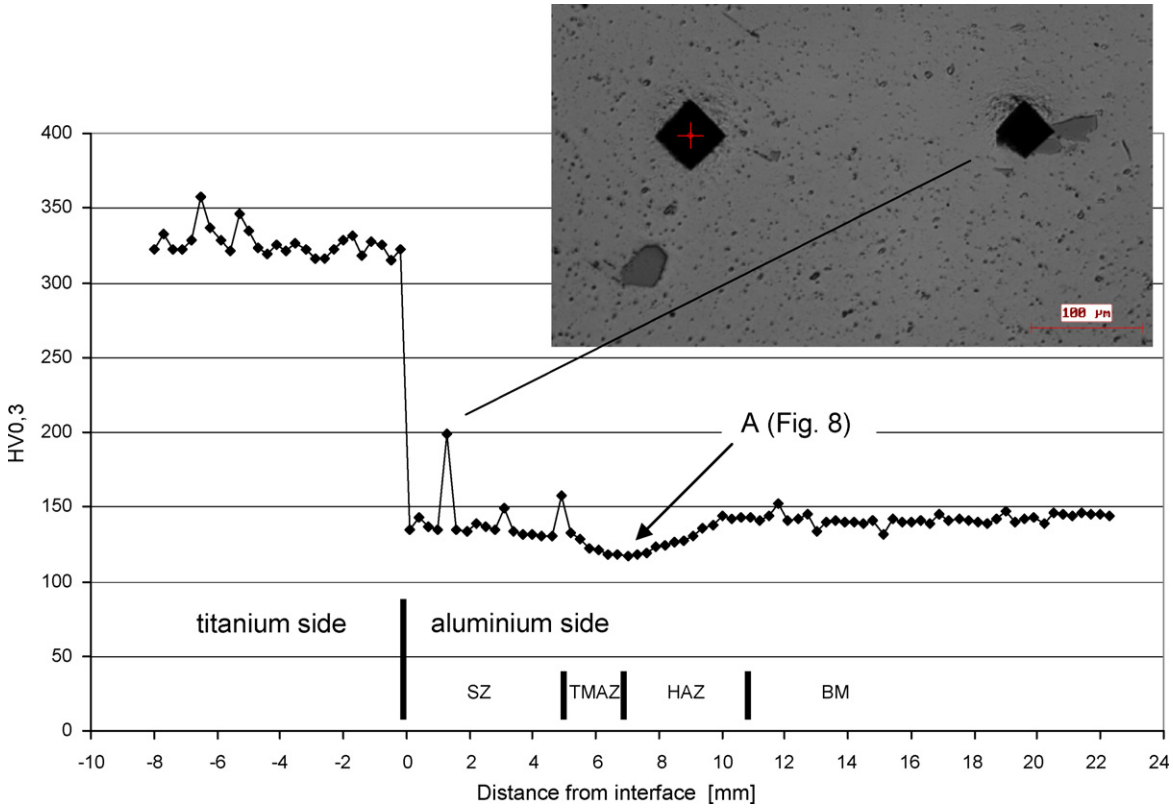

Fig. 6. Hardness profile of cross-section taken perpendicular to welding direction.

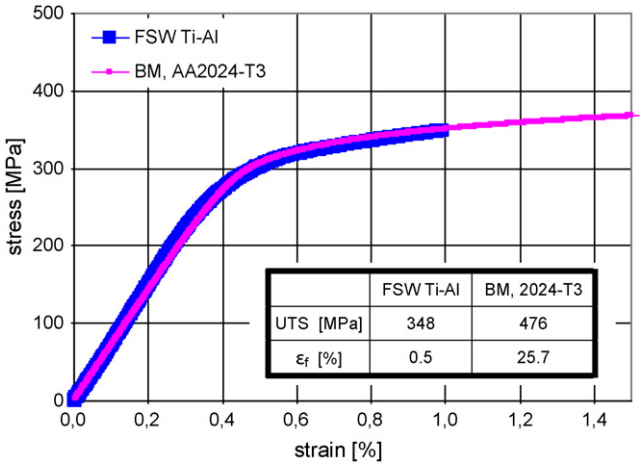

Fig. 7. Stress–strain curves of FSW-joint and base material AA2024-T3.

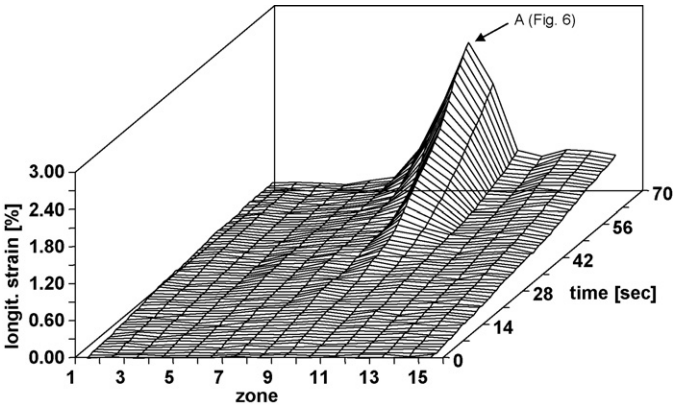

Fig. 8. Local elongation as registered by laser extensometry in the course of a tensile test.

tion zone on the aluminium side of the joint (Fig. 8) exactly at the position the absolute hardness minimum is localized (point A in Fig. 6). Nevertheless, the fracture zone is not situated at the place of highest local elongation, but at the interface between titanium and aluminium. This apparent contradiction can be solved by the following consideration: In the initial phase of a tensile test there is only elastic deformation distributed over the joint according to the different Young's moduli of both materials, but resulting differences in elastic strain of about 0.15% are too small to be resolved by the laser extensometer. As soon as the local yield strength of the TMAZ/HAZ transition zone on the aluminium side of the joint is exceeded, further plastic deformation is restricted to that location. In the following, work hardening starts to strengthen that low-strength region allowing for further increasing the nominal load. At ca. 348 MPa, the strength of the titanium–aluminium interface is reached inducing final fracture without any additional plastic elongation in that area.

Since no intermediate layer could be found for the most part of the interface (exemplarily Fig. 5), the main bonding mechanism of the interface is assumed to be diffusion bonding. However, there are some areas on the fracture surface, where the aluminium alloy was still bonded to titanium. Fig. 9 demonstrates by EDX profiles, that these areas display an aluminium content of about 90%. A larger magnification of these zones shows a typical ductile fracture surface of aluminium being characterized by the presence of dimples (Fig. 10). These aluminium particles bonded to the titanium demonstrate that the welding connection is very strong at these zones. The mechanism of bonding in these zones is exposed more

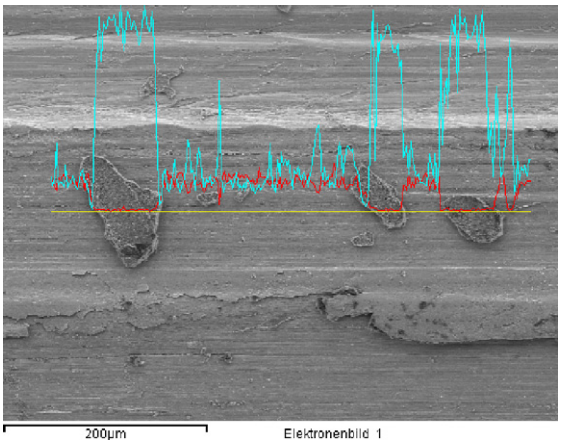

Fig. 9. Fracture surface (titanium side) with adhesive aluminium spots; EDX-colours: red (dark) → titanium, blue (light) → aluminium. (For interpretation of the references to colour in this figure legend, the reader is referred to the web version of the article.)

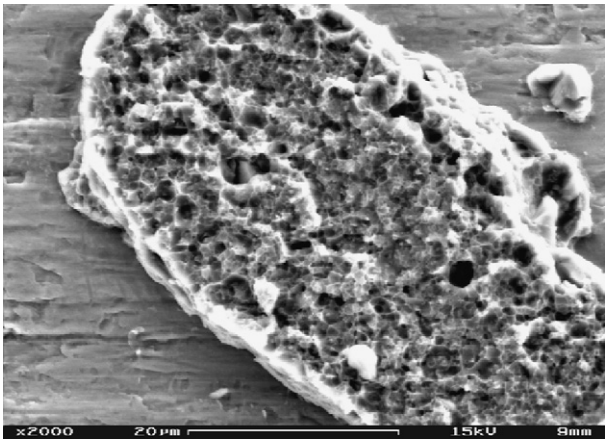

Fig. 10. Dimples at aluminium spots.

closely in Fig. 11. A swirl-like structure with lighter and darker parts was observed in the SEM micrograph of the interface region. One material is clutched into the other demonstrating intimate contact. (Fig. 12 gives a lower magnification picture of such a region.) First,

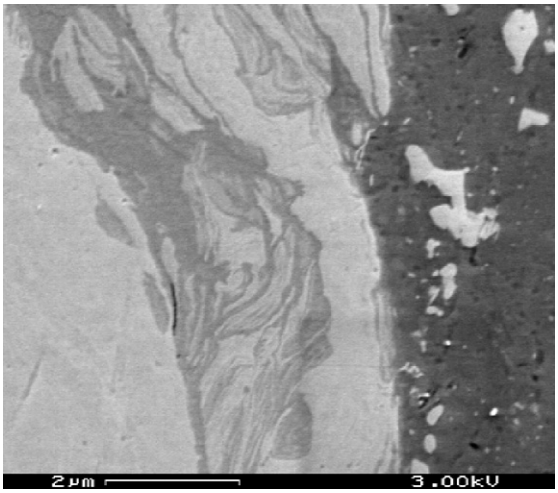

Fig. 11. Cross-section of interface region light parts → titanium, dark parts → aluminium.

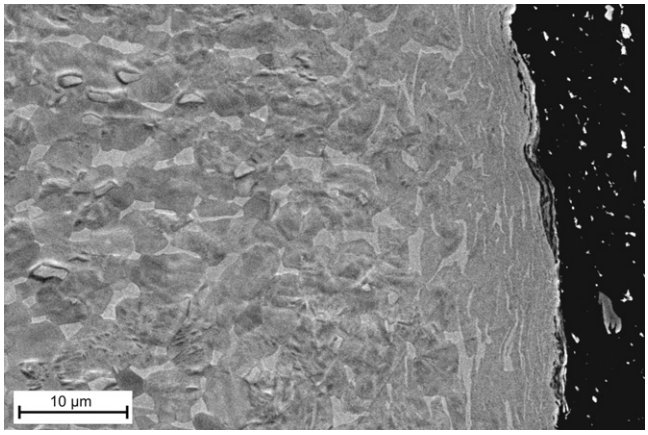

Fig. 12. Overview of interface region with swirl-like structure (SEM-picture).

this might indicate a kind of local micro-mechanical bonding mechanism. But second, an additional chemical bonding mechanism is assumed to strengthen the interface in the areas where aluminium was still bonded to titanium. The different grey scales in Fig. 11 suggest the formation of an intermetallic phase (possibly $TiAl_2$). These Ti_xAl_x-phases are indeed known to be brittle, but in this case their thickness could be restricted to 1 μm in maximum. Therefore the intermetallic film might have acted as an adhesion-promoting agent, because the areas with swirl-like structure seem to be the areas with the highest bond strength.

The tensile test also reveals the quality of adhesion between titanium particles and the aluminium matrix in the SZ. While there is no lack of adhesion visible in the cross-section of Fig. 2 (nor in larger magnification (not pictured)), there are some small openings between titanium particles and the aluminium matrix after tensile testing (Fig. 13). However, these sporadic openings are not caused by a deficit of adhesion, but by a compensation of the strain mismatch between aluminium and titanium. During the elongation in the course of the tensile test, the titanium particles elongate in a smaller extent than the surrounding aluminium matrix causing the formation of cavities at the edge of the titanium particles. Another indication of the strain mismatch is the fact that these openings preferably occur on the small side of particles, which are orientated in loading direction.

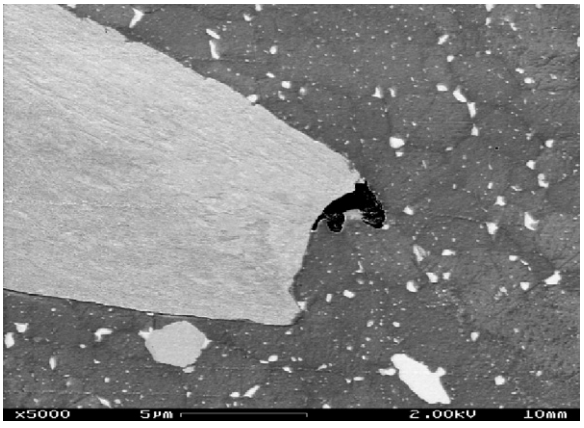

Fig. 13. Cross-section of specimen after tensile test; light parts → titanium particles in SZ; direction of tensile test: left ↔ right.

4. Summary

The feasibility of friction stir welding dissimilar materials (TiAl6V4 and AA2024-T3) and the properties of these joints were investigated. Unlike the conventional friction stir butt welding, the tool pin centre was shifted towards the aluminium plate. Therefore the aluminium side shows the characteristics of a conventional friction stir weld concerning microstructure and distribution of hardness, except some titanium particles in the stirred zone. On the titanium side of the joint, a small band next to the titanium–aluminium interface has recrystallized. The ultimate tensile strength of the joints reached 73% of AA2024-T3 base material strength. Highest local elongation occurred, as expected, on the aluminium side of the joint in the region, where the hardness minimum was localized. But the fracture surface is situated at the interface between titanium and aluminium. However, there are some areas on the fracture surface, where the aluminium alloy was still bonded to titanium. It is assumed that these areas correspond with swirl-like structures observed on metallographic sections, which depict that one material was clutched into the other at least locally. The main objective of future research might be the increase in number and size of these clutched areas by optimization of welding parameters.

Acknowledgements

The authors thank Mr. Sauer for friction stir welding the aluminium titanium joints and Mr. Fuchs for conducting the tensile tests.

References

[1] W. Zink, in: M. Peters, W.A. Kaysser (Eds.), Advanced Aerospace Materials, DGLR, Munich, Germany, 2000, pp. 25–32.
[2] J. Wilden, J.P. Bergmann, Welding and Cutting 3 (2004) 285–290.
[3] A.A. Osokin, Welding Production 23 (1976) 18–20.
[4] M. Kreimeyer, F. Wagner, F. Vollertsen, Optics and Lasers in Engineering 43 (2005) 1021–1035.
[5] A. Fuji, Science and Technology of Welding and Joining 7 (2002) 413–416.
[6] W.M. Thomas, E.D. Nicholas, J.C. Needham, M.G. Murch, P. Templesmith, C.J. Dawes, Improvements Relating to Friction Welding, European Patent, EP 0 615 480 B1 (1992).
[7] Y.C. Chen, K. Nakata, Materials & Design 30 (2009) 469–474.
[8] H. Uzun, C. Dalle Donne, A. Argagnotto, T. Ghidini, C. Gambaro, Materials & Design 26 (2005) 41–46.
[9] W.-B. Lee, M. Schmuecker, U. Alfaro Mercado, G. Biallas, S.-B. Jung, Scripta Materialia 55 (2006) 355–358.
[10] R.S. Coelho, A. Kostka, J.F. Dos Santos, A.R. Pyzalla, Advanced Engineering Materials 10 (2008) 1127–1133.
[11] G. Biallas, C. Dalle Donne, Materialprüfung, Jahrg. 42 (6) (2000) 236–239.
[12] G. Biallas, R. Braun, C. Dalle Donne, G. Staniek, W.A. Kaysser, 1st International Symposium on Friction Stir Welding, Thousand Oaks, CA, USA, 1999.
[13] Y. Sato, H. Kokawa, M. Enomoto, S. Jogan, Metallurgical and Materials Transactions A 30 (1999) 2429–2437.
[14] Z.Y. Ma, R.S. Mishra, M.W. Mahoney, Acta Materialia 50 (2002) 4419–4430.
[15] M. Peters, J. Hemptenmacher, J. Kumpfert, C. Leyens, in: M. Peters, C. Leyens (Eds.), Titan und Titanlegierungen, Wiley-VCH, 2002, pp. 1–37.
[16] C. Genevois, A. Deschamps, A. Denquin, B. Doisneau-Cottignies, Acta Materialia 53 (8) (2005) 2447–2458.
[17] Y.S. Sato, M. Urata, H. Kokawa, K. Ikeda, Materials Science and Engineering A 354 (1–2) (2003) 298–305.
[18] C. Dalle Donne, R. Braun, G. Staniek, A. Jung, W.A. Kaysser, Zeitschrift für Metallkunde 29 (29) (1998) 609–617.
[19] E.B.F. Lima, J. Wegener, C. Dalle Donne, G. Goerigk, T. Wroblewski, T. Buslaps, A.R. Pyzalla, W. Reimers, Zeitschrift für Metallkunde 94 (8) (2003) 908–915.
[20] C. Dalle Donne, G. Biallas, DVM-Bericht 231 (1999) 53–61.
[21] C. Dalle Donne, H. Döker, Friction Stir Welding von Luft- und Raumfahrtstrukturen: Der Prozess und die Eigenschaften, Deutscher Luft- und Raumfahrtkongress 2003, DGLR Jahrbuch, 2003, pp. 725–731.